Polymer Journal (2010) 42, 494–500

www.nature.com/pj

ORIGINAL ARTICLE

Selective preparation of novel fluoroalkyl end-capped co-oligomeric nanocomposite-encapsulated magnetites and magnetite-adsorbing co-oligomeric nanoparticles

Hideo Sawada, Tetsushi Kijima and Masaki Mugisawa

New crosslinked fluoroalkyl end-capped co-oligomeric nanocomposite-encapsulated magnetic nanoparticles, prepared by the deprotecting reactions of corresponding fluorinated co-oligomers containing oxime-blocked segments in the presence of magnetic nanoparticles, were produced with nanometer-scale diameters (with diameters in the range of 154–192 nm). The nanoparticles exhibited good dispersibility in traditional organic solvents. They were applied as a surface modification to poly(methyl methacrylate), resulting in good oleophobicity imparted by the fluorine and magnetic properties arising from the encapsulated magnetic nanoparticles. Fluoroalkyl end-capped 2-acrylamido-2-methylpropanesulfonic acid co-oligomers containing adamantane segments form nanometer-sized controlled fine particles in methanol and can interact with magnetic nanoparticles to form fluorinated betaine-type co-oligomeric nanocomposite-encapsulated magnetic nanoparticles (with an average particle size of 25–183 nm). These fluorinated betaine-type nanocomposite-encapsulated magnetic nanoparticles exhibit the lower critical solution temperature (LCST) characteristic in organic media such as *t*-butyl alcohol and were found to effectively decrease the LCST through the encapsulation of magnetic nanoparticles in fluorinated co-oligomeric nanoparticle cores. Interestingly, transmission electron microscopy images show that magnetic nanoparticles can be encapsulated inside the crosslinked fluorinated co-oligomeric nanocomposite cores; in contrast, magnetic nanoparticles are adsorbed on the surface of fluorinated betaine-type co-oligomeric nanocomposite cores.
Polymer Journal (2010) **42,** 494–500; doi:10.1038/pj.2010.27; published online 21 April 2010

Keywords: adsorption; encapsulation; fluorinated co-oligomeric nanoparticle; LCST; magnetite; surface modification; TEM

INTRODUCTION

Much attention has been devoted recently to well-dispersed magnetic colloidal particles, owing to the broad range of potential applications in the fields of ferrofluids,[1,2] high-density data storage,[3] disks and toner in printing,[4–6] magnetic resonance imaging,[7,8] enzyme immobilization,[9] rapid biological separation,[10,11] drug delivery,[12–14] biomedical materials,[15–17] immunoassays[18,19] and biosensors.[20,21] The development of colloidal-stable magnetic nanoparticles is essential from a practical point of view. The surface functionality of magnetic nanoparticles with functionalized polymers can form colloidal-stable magnetic nanoparticles. So far, numerous synthetic and natural polymers have been used to obtain stable colloidal dispersions of magnetic nanoparticles by coating and encapsulating the particles.[22–31] It is well known that fluorinated surfactants have excellent surface characteristics, including oleophobicity and hydrophobicity, neither of which can be achieved with corresponding nonfluorinated polymers.[32] Thus, it is of particular interest to develop new, tailored magnetic fluorinated polymer colloids that possess not only good dispersibility in various solvents but also the unique active surface characteristics imparted by fluorine. In fact, we have already reported that fluoroalkyl end-capped oligomers containing not only carboxyl groups but also other functional groups such as phosphonic acid, sulfonic acid and sulfobetaine-type groups can interact effectively with the residual hydroxyl groups on the magnetite surface to form new fluorinated magnetic nanocomposites with good dispersibility in a variety of solvents, including water.[33–36] Such good dispersibility of tailored magnetic fluorinated polymer colloids is due to the presence of fluoroalkyl end-capped oligomers because fluoroalkyl end-capped oligomers can exhibit various unique properties such as high solubility, surface active properties, biological activities and nanometer scale self-assembled molecular aggregates, which cannot be achieved by the corresponding nonfluorinated, randomly fluoroalkylated and AB block-type fluoroalkylated polymers.[37–40] With regard to these fluoroalkyl end-capped oligomers, we have very recently found that crosslinked fluoroalkyl end-capped co-oligomers containing both oxime-blocked isocyanato and hydroxy adamantyl segments can

Department of Frontier Materials Chemistry, Graduate School of Science and Technology, Hirosaki University, Hirosaki, Japan
Correspondence: Dr H Sawada, Frontier Materials Chemistry, Hirosaki University, 3 Bunkyo-cho, Hirosakai 036-8561, Japan.
E-mail: hideosaw@cc.hirosaki-u.ac.jp
Received 20 December 2009; revised 23 February 2010; accepted 24 February 2010; published online 21 April 2010

form new crosslinked fluoroalkyl end-capped co-oligomeric nanoparticles containing adamantane segments through the deprotecting reaction of oxime-blocked isocyanato segments in co-oligomers.[41,42] We have also found that fluoroalkyl end-capped 2-acrylamido-2-methylpropanesulfonic acid co-oligomers containing adamantane segments can form nanometer-scale particles, not only in water but also in various traditional organic solvents.[43,44] The architecture of such fluorinated fine nanoparticles is because of the moderate oleophilic–oleophobic balance in these co-oligomeric nanoparticles, corresponding to the oleophilic character of the bulky adamantyl segments and the oleophobic character of end-capped fluoroalkyl groups.[41–44] Therefore, it is expected that these fluorinated co-oligomeric nanoparticle cores should interact with magnetic nanoparticles as a guest molecule to form colloidal-stable fluorinated co-oligomeric nanocomposite-encapsulated magnetic particles. Here, we report that magnetic nanoparticles can be encapsulated into crosslinked fluoroalkyl end-capped co-oligomeric nanoparticle cores containing adamantyl segments to form colloidally stable magnetic nanoparticles. We place particular emphasis on the applications of these nanocomposites as surface modifications for traditional organic polymers, providing both good oleophobicity due to the end-capped fluoroalkyl groups and also magnetic properties arising from the presence of magnetic nanoparticles. In fluorinated betaine-type co-oligomeric nanoparticles, we have found that these fluorinated nanoparticles can effectively decrease the LCST (lower critical solution temperature) in *t*-butyl alcohol through the adsorption of magnetic nanoparticles outside the fluorinated particle cores. These results are described herein.

EXPERIMENTAL PROCEDURE

Measurements

Nuclear magnetic resonance spectra were measured using a JEOL JNM-400 (400 MHz) FT NMR SYSTEM (Tokyo, Japan). Ultraviolet-visible spectra were measured using a Shimadzu UV-1600 UV-vis spectrophotometer (Kyoto, Japan). Dynamic light-scattering (DLS) measurements were taken using an Otsuka Electronics DLS-7000 HL system (Tokyo, Japan). Thermal analyses were recorded on a Bruker axs TG-DTA2000SA differential thermobalance (Kanagawa, Japan). Contact angles were measured using Kyowa Interface Science Drop Master 300 (Saitama, Japan). Transmission electron microscopy (TEM) was conducted using a JEOL JEM-1210 Electron microscope.

Materials

Isocyanatoethyl methacrylate 2-butanone oxime adduct (IEM-BO) was obtained from Showa Denko (Tokyo, Japan). 1-hydroxy-5-adamantylacrylate (Ad-HAc) and magnetic nanoparticles (with an average particle size of 10 nm) were used as received from Idemitsu Kosan (Tokyo, Japan) and Toda Kogyo Corporation (Hiroshima, Japan), respectively. We purchased 2-acrylamido-2-methylpropanesulfonic acid from Tokyo Kasei Kogyo.

Preparation of crosslinked fluoroalkyl end-capped co-oligomeric nanocomposite-encapsulated Magnt

A typical procedure for the preparation of crosslinked fluoroalkyl end-capped co-oligomeric nanocomposite-encapsulated **Magnt** by the use of α,ω-bis(perfluoro-1-methyl-2-oxapentylated) isocyanatoethyl methacrylate 2-butanone oxime adduct–1-hydroxy-5-adamantylacrylate co-oligomers [R_F-(IEM-BO)$_x$-(Ad-HAc)$_y$-R_F; R_F=$CF(CF_3)OC_3F_7$; *x*:*y*=21:79; *M*n=2600] is as follows: magnetic nanoparticles (200 mg, with an average particle size of 10 nm) were added to an *N*,*N*-dimethylformamide (25 ml) solution of R_F-(IEM-BO)$_x$-(Ad-HAc)$_y$-R_F co-oligomer (1.0 g), which was prepared by co-oligomerization of the corresponding monomers and fluoroalkanoyl peroxide according to our previously reported method.[41,42] The mixture was stirred at room temperature for 2 days under ultrasonic irradiation conditions and then stirred with a magnetic bar at 130 °C for 1 h. Methanol (20 ml) was added to the reaction mixture, and the mixture was stirred well for 30 min at room temperature. After the centrifugal separation (2000 r.p.m./30 min) at room temperature, the supernatant solution was evaporated under reduced pressure. The isolated crude product was reprecipitated from methanol–acetone to yield purified crosslinked fluorinated co-oligomeric nanocomposite-encapsulated **Magnt** (828 mg). The nanocomposite particles exhibited the following Fourier transform infrared spectrum characteristics, with features corresponding to the presence of magnetic nanoparticles: infrared (cm^{-1}) 560. Other R_F-(IEM)$_x$-(Ad-HAc)$_y$-R_F co-oligomeric nanocomposite-encapsulated **Magnt** were prepared under similar conditions.

Preparation of fluoroalkyl end-capped betaine-type co-oligomeric nanocomposite-encapsulated Magnt

A typical procedure for the preparation of fluoroalkyl end-capped betaine-type co-oligomeric nanocomposite-encapsulated **Magnt** by the use of α,ω-bis(perfluoro-1-methyl-2-oxapentylated) 2-acrylamido-2-methylpropane sulfonic acid–1-hydroxy-5-adamantylacrylate co-oligomer [R_F-(AMPS)$_x$-(Ad-HAc)$_y$-R_F; R_F=$CF(CF_3)OC_3F_7$; *x*:*y*=44:56 (the molecular weight of this co-oligomer cannot be determined by size exclusion chromatography because of the formation of nanoparticles)] is as follows: magnetic nanoparticles (15 mg; with an average particle size of 10 nm) were added to a methanol (25 ml) solution of R_F-(AMPS)$_x$-(Ad-HAc)$_y$-R_F co-oligomer (150 mg), which was prepared by the co-oligomerization of the corresponding monomers and fluoroalkanoyl peroxide according to our previously reported method.[43,44] The mixture was stirred at room temperature for 6 h under ultrasonic irradiation conditions. After centrifugal separation (2000 r.p.m./30 min) at room temperature, the supernatant solution was evaporated under reduced pressure to yield purified fluorinated betaine-type co-oligomeric nanocomposite-encapsulated **Magnt** (112 mg). These nanocomposite particles exhibited the following Fourier transform infrared spectrum characteristics, with features corresponding to the presence of magnetic nanoparticles: infrared (cm^{-1}) 560. Other R_F-(AMPS)$_x$-(Ad-HAc)$_y$-R_F co-oligomeric nanocomposite-encapsulated **Magnt** were prepared under similar conditions.

Preparation of PMMA-modified film treated with crosslinked fluoroalkyl end-capped co-oligomeric nanocomposite-encapsulated Magnt

The poly(methyl methacrylate) (PMMA)-modified film (with a film thickness of 194 μm) was prepared by casting mixed solutions of methanol and 1,2-dichloroethane (v/v=5/20; 25 ml total volume) containing PMMA (990 mg) and crosslinked R_F-(IEM)$_x$-(Ad-HAc)$_y$-R_F co-oligomeric nanocomposite-encapsulated **Magnt** (Run 4 in Table 1; 10 mg) on a glass plate. The solvent was evaporated at room temperature, and the resulting film was peeled off and dried at 50 °C for 24 h under vacuum to obtain the PMMA-modified film. Contact angles for dodecane on both the surface and the reverse sides of the modified film were measured at room temperature using a goniometer.

Measurements of the LCST of fluoroalkyl end-capped betaine-type co-oligomeric nanocomposite-encapsulated Magnt

The LSCTs of R_F-(AMPS)$_x$-(Ad-HAc)$_y$-R_F co-oligomeric nanocomposite-encapsulated **Magnt** in *t*-butyl alcohol were measured using a turbidity method. A ultraviolet-visible spectrophotometer equipped with a temperature controller was used to trace the phase transition by monitoring the transmittance of light at a wavelength of 500 nm as a function of temperature. The concentration of the co-oligomeric nanocomposite solutions used was 4 g dm^{-3}, and LCST was defined as the temperature at which the transmittance was 50%.

RESULTS AND DISCUSSION

Preparation and characteristics of novel crosslinked fluoroalkyl end-capped co-oligomeric nanocomposite-encapsulated magnetic nanoparticles

The deprotecting reactions of fluoroalkyl end-capped isocyanatoethyl methacrylate 2-butanone oxime adduct–1-hydroxy-5-adamantylacrylate co-oligomers [R_F-(IEM-BO)$_x$-(Ad-HAc)$_y$-R_F] were carried out in *N*,*N*-dimethylformamide in the presence of magnetic nanoparticles

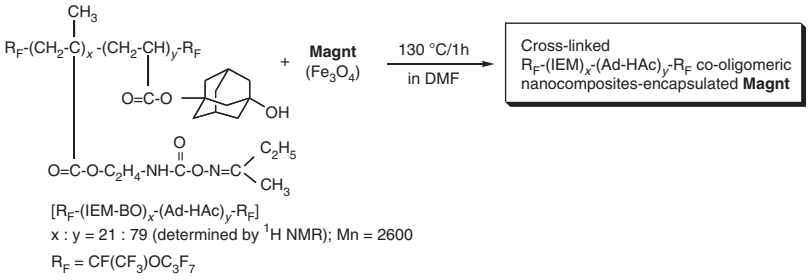

Scheme 1 R_F-(IEM)$_x$-(Ad-HAc)$_y$-R_F co-oligomeric nanocomposite-encapsulated **Magnt**.

Table 1 Preparation of crosslinked R_F-(IEM)$_x$-(Ad-HAc)$_y$-R_F co-oligomeric nanocomposite-encapsulated Magnt

Run	*R_F-(IEM-BO)$_x$-(Ad-HAc)$_y$-R_F (g)*	***Magnt** (size: 10 nm) (mg)*	*Product yield*[a] *(%)*	*Size of dispersed nanocomposites in methanol*[b,c]	*Contents of **Magnt** in nanocomposites (%)*
1	1.0	20	57	154 ± 31	4
2		50	61	175 ± 50	5
3		100	64	168 ± 35	10
4		200	69	192 ± 40	20
5		400	62	168 ± 40	26
6		600	71	186 ± 39	41
7		800	43	279 ± 54	38
8		1000	42	304 ± 45	31

[a]Yields were based on R_F-(IEM-BO)$_x$-(Ad-HAc)$_y$-R_F and **Magnt**.
[b]Determined by dynamic light scattering measurements.
[c]Size of parent R_F-(IEM-BO)$_x$-(Ad-HAc)$_y$-R_F co-oligomeric nanoparticles: 11 ± 1.1 nm.

(**Magnt**; with a mean diameter of 10 nm) at 130 °C for 1 h, and the results are shown in Scheme 1 and Table 1.

As shown in Scheme 1 and Table 1, the deprotecting reactions were found to proceed under mild conditions to form a variety of crosslinked fluoroalkyl end-capped co-oligomeric nanocomposite-encapsulated **Magnt** in isolated yields of 42–69%. The obtained crosslinked fluorinated co-oligomeric nanoparticle-encapsulated **Magnt** exhibited good dispersibility in methanol, tetrahydrofuran, dimethyl sulfoxide and *N*,*N*-dimethylformamide. We measured the size of crosslinked fluorinated nanocomposite-encapsulated **Magnt** in methanol solutions using DLS at a temperature of 30 °C. These results are also shown in Table 1.

The size (number-average diameter) of these fluorinated particles ranged from approximately 154 to 304 nm and were monodispersed. The size of these fluorinated nanocomposite-encapsulated **Magnt** was found to increase from approximately 11 nm to 154–304 nm after the encapsulation of **Magnt**. The size increase of the nanocomposites indicates that the encapsulations of **Magnt** proceeded smoothly toward the synthesis of very fine crosslinked fluorinated co-oligomeric nanocomposite-encapsulated **Magnt**.

The contents of encapsulated **Magnt** in crosslinked fluorinated co-oligomeric nanoparticles were estimated by thermogravimetric analyses. In this process, the weight loss of nanocomposites was measured as the temperature was increased at a heating rate of 10 °C min^{-1} to a maximum temperature of 800 °C under atmospheric conditions. The thermal stability of crosslinked fluorinated nanocomposite-encapsulated **Magnt** was inferior to that of the parent magnetic nanoparticles. In addition, the original R_F-(IEM-BO)$_x$-(Ad-HAc)$_y$-R_F co-oligomer was found to completely decompose around 550 °C. These results imply that the **Magnt** contents range from 4 to 41% for the different samples, as listed in Table 1.

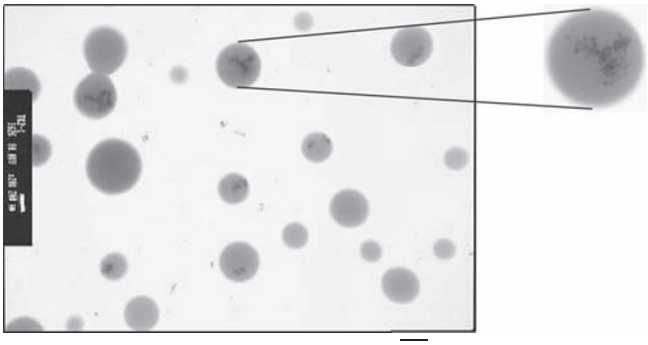

Figure 1 TEM image of crosslinked fluorinated co-oligomeric nanocomposite-encapsulated **Magnt** (Run 2 in Table 1) in methanol.

X-ray diffraction patterns of fluorinated crosslinked nanocomposite-encapsulated **Magnt** and parent **Magnt** were similar. However, the collected diffraction intensity was extremely weakened for the fluorinated nanoparticles possessing lower encapsulated ratios of **Magnt** (Runs 1 and 2 in Table 1). The Fourier transform infrared spectrum peak near 560 nm that was present for each fluorinated crosslinked nanocomposite implies the presence of encapsulated **Magnt** in the fluorinated crosslinked nanoparticle cores.

To confirm the presence of encapsulated **Magnt** in the fluorinated nanoparticle cores, we examined a methanol solution of crosslinked fluorinated co-ologomeric nanocomposite-encapsulated **Magnt** listed as Run 2 in Table 1 using TEM. The TEM micrograph is shown in Figure 1.

The electron micrograph also shows the formation of crosslinked fluorinated nanocomposite-encapsulated magnetic fine particles, showing a mean nanoparticle diameter of 262 nm. This is similar to the number-average diameter of 175–50 nm found in DLS measurements, shown in Table 1. Interestingly, TEM photographs show that the amounts of **Magnt** encapsulated into fluorinated composite cores can increase quite effectively with increasing **Magnt** content in the nanocomposites from 4 to 20% (see Figure 2).

As shown in Figure 3, colloidal-stable magnetic particles were obtained in methanol solutions even under the following conditions: (a) centrifugal separation for 30 min (b) 60 min at 3000 r.p.m. and (c) at room temperature. To investigate the magnetic response of the colloidal-stable fluorinated nanocomposites in methanol solution against an external magnetic field, a permanent magnet was applied from the bottom of the sample tube containing this methanol solution (see Figure 3d–f). This nanocomposite exhibited good dispersibility in methanol (Figure 3d); however, the composite instantaneously precipitated on application of the magnet (Figure 3e). We succeeded in preparing a redispersed colloidal-stable nanocomposite solution after the magnet application (Figure 3f)) that was similar to the original one (Figure 3d). This behavior indicates that the fluorinated magnetic nanocomposites still maintain their ferromagnetism.

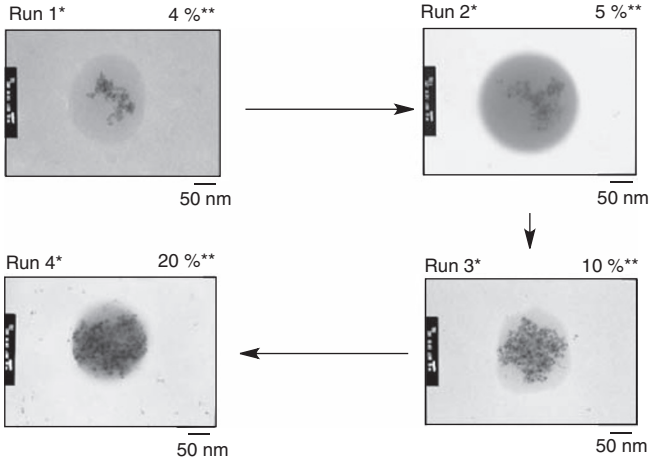

Figure 2 TEM photographs of a variety of crosslinked fluorinated co-oligomeric nanocomposite-encapsulated **Magnt** in methanol. *Each different from those of Table 1. **Contents of **Magnt** in the composites determined by thermogravimetric analyses.

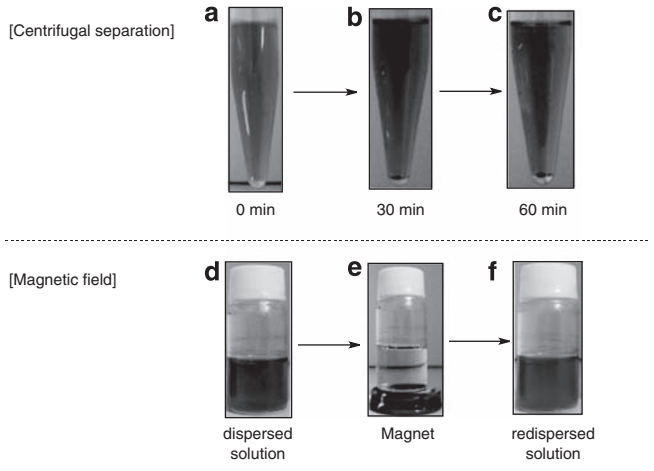

Figure 3 Photographs of R_F-$(IEM)_x$-$(Ad\text{-}HAc)_y$-R_F co-oligomeric nanocomposite-encapsulated **Magnt** (Run 4 in Table 1) in methanol (concentration of nanocomposites in methanol: 1 g dm^{-3}).

Application of novel crosslinked fluoroalkyl end-capped co-oligomeric nanocomposite-encapsulated magnetic nanoparticles to the surface modification of traditional organic polymers

In this way, our present crosslinked fluorinated nanocomposite-encapsulated **Magnt** are very fine particles and have good dispersibility in a variety of organic media. Thus, it is of particular interest to apply these fluorinated nanocomposites as a surface modification for organic polymers such as PMMA. We have prepared a PMMA-modified film by casting homogeneous solutions of PMMA and fluorinated nanocomposites in tetrahydrofuran (Runs 1–8, listed in Table 1). The contact angles of dodecane on the surface and reverse sides of the modified brown-colored PMMA films were measured, and the results are shown in Table 2. Film thickness ranged from 187 to 199 μm.

As shown in Table 2, for each film, higher dodecane contact angles for dodecane on the surface side compared with the reverse side were obtained in each modified film, suggesting that fluorinated nanocomposites could be arranged on the polymer surface to exhibit strong oleophobicity because of end-capped fluoroalkyl segments on the surface. Interestingly, as shown in Figure 4, the PMMA-modified film treated with fluorinated nanocomposites (Run 4 in Table 1) was found to interact with a permanent magnet, indicating that this modified polymer possesses not only oleophobic characteristics but also ferromagnetism.

Table 2 Contact angles of dodecane on the modified PMMA films, treated with crosslinked fluorinated co-oligomeric nanocomposite-encapsulated Magnt

		Contact angle (degree)		
		Dodecane		
Run[a]	*Contents of **Magnt**[b] (%)*	*Surface side*	*Reverse side*	*Film thickness (μm)*
1	4	11	0	187
2	5	22	0	192
3	10	19	0	199
4	20	13	0	194
5	26	21	0	196
6	41	14	0	190
7	38	13	0	195
8	31	14	0	193

[a]Each different from those in Table 1.
[b]Contens of **Magnt** in the nanocomposites were determined by thermogravimetric analyses.

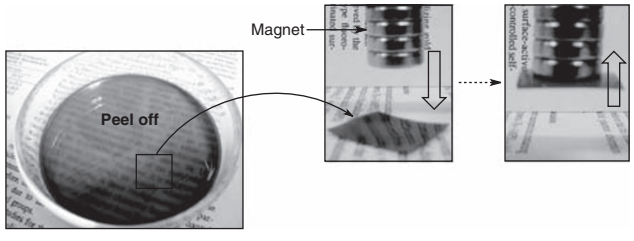

PMMA cast film*) treated with R_F-$(IEM)_x$-$(Ad\text{-}HAc)_y$-R_F co-oligomeric nanocomposites-encapsulated **Magnt** (Run 4 in Table 1)

Figure 4 Photographs of modified PMMA films treated with crosslinked fluorinated nanocomposite-encapsulated magnetic nanoparticles. *Concentration of R_F-$(IEM)_x$-$(Ad\text{-}HAc)_y$-R_F co-oligomeric nanocomposite-encapsulated **Magnt** based on PMMA is 3% (m/m).

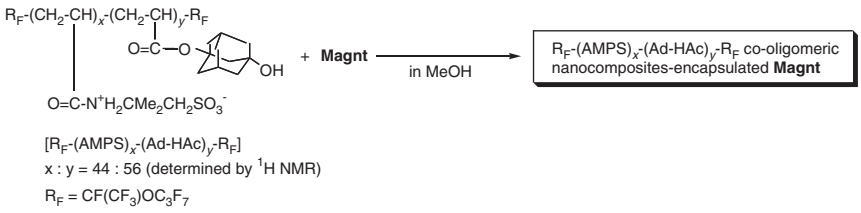

Scheme 2 R_F-$(AMPS)_x$-$(Ad$-$HAc)_y$-R_F co-oligomeric nanocomposite-encapsulated **Magnt**.

Table 3 Preparation of fluorinated betaine-type co-oligomeric nanocomposite-encapsulated Magnt

Run	*R_F-(IEM-BO)$_x$-(Ad-HAc)$_y$-R_F (mg)*	***Magnt** (mg)*	*Product yields[a] (%)*	*Size of dispersed nanocomposites[b,c] (nm)*	*Size of dispersed nanocomposites[b,c] (nm)*	*Contents of **Magnt** in nanocomposites (%)*
9	150	5	59	36 ± 2.3	124 ± 12	2
10		15	68	58 ± 7.0	110 ± 11	13
11		30	64	183 ± 41	80 ± 4.6	10
12		60	49	25 ± 2.5	99 ± 13	19
13		100	44	57 ± 9.6	136 ± 22	17
14		150	34	49 ± 5.0	101 ± 22	16

[a]Yields were based on R_F-$(AMPS)_x$-$(Ad$-$HAc)_y$-R_F and **Magnt**.
[b]Determined by dynamic light scattering measurements in methanol.
[c]Size of parent R_F-$(AMPS)_x$-$(Ad$-$HAc)_y$-R_F co-oligomeric nanoparticles: 17 ± 2.5 nm.

Preparation and characteristics of novel crosslinked fluoroalkyl end-capped betaine-type co-oligomeric nanocomposite-encapsulated magnetic nanoparticles

We attempted to encapsulate magnetic nanoparticles into fluoroalkyl end-capped co-oligomeric betaine-type nanoparticle cores. In fact, we succeeded in preparing fluorinated betaine-type co-oligomeric nanocomposite-encapsulated **Magnt** in isolated yields of 34–68% by the treatment of corresponding fluorinated betaine-type co-oligomeric nanoparticles with **Magnt** in methanol under ultrasonic irradiation conditions, as shown in Scheme 2 and Table 3.

The **Magnt** content in the nanocomposites in Table 3 was estimated to be between 2 and 19% using thermogravimetric analyses. The **Magnt** content was found to increase when the feed amount of **Magnt** was increased from 5 to 150 mg. Above a feed amount of 60 mg, the **Magnt** content of the particles remained fairly constant, between 16 and 19% (see Table 3). DLS measurements revealed that the size of nanocomposite particles increased from 17 nm (the number-average diameter size of parent fluorinated co-oligomeric nanoparticles) to between 25 and 183 nm in methanol after the composite reactions, indicating that **Magnt** was effectively encapsulated into the fluorinated co-oligomeric nanoparticle cores (see Table 3). Interestingly, these fluorinated nanocomposite-encapsulated **Magnt** exhibited good dispersibility and redispersibility in methanol. The size (80–136 nm) of the redispersed fluorinated nanocomposite particles did not change, even after redispersion of the parent fluorinated nanocomposite-encapsulated **Magnt** powders (with diameters between 25 and 183 nm) in methanol. The size distributions of each nanocomposite were monodispersed (see Table 3).

To confirm the presence of encapsulated **Magnt** in fluorinated co-oligomeric nanoparticle cores, we took TEM images of a methanol solution of the fluorinated beanie-type co-oligomeric nanocomposite-encapsulated **Magnt** (Run 9 in Table 3). The resulting micrographs are shown in Figure 5.

The electron micrograph shows the formation of fine particles of fluorinated nanocomposite-encapsulated **Magnt**, with mean diameters of 126 nm (Figure 5). The particle diameters measured through TEM are quite similar to the values determined from DLS measurements (which gave number-average diameters of 124–12 nm for redispersed nanocomposites, Run 9 in Table 3).

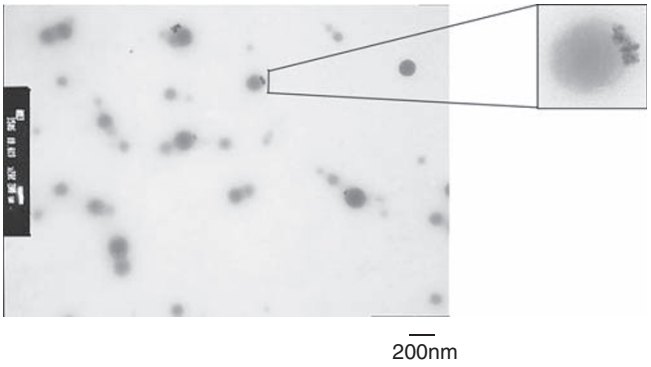

Figure 5 TEM image of **Magnt** adsorbed on fluorinated betaine-type co-oligomeric nanocomposites (Run 9 in Table 3).

Surprisingly, the encapsulation behavior of magnetic nanoparticles into fluorinated co-oligomeric nanoparticle cores, shown in Figure 5, is quite different from that of fluorinated crosslinked nanocomposite-encapsulated **Magnt**, shown in Figures 1 and 2. In fluorinated betaine-type co-oligomeric nanocomposites, magnetic nanoparticles are adsorbed outside the co-oligomeric particle cores through the effective covalently binding interaction between the sulfobetaine-type segments in co-oligomers and the residual hydroxyl groups in magnetic particles. In fact, it has already been reported that carboxy,[45] sulfo,[46] phosphate[47] and phosphoric[48,49] groups can interact with magnetic nanoparticles through covalent bonds. No covalent binding interactions in crosslinked fluorinated co-oligomeric nanoparticles (in Scheme 1) should allow the encapsulation of magnetic nanoparticles inside fluorinated co-oligomeric particle cores through the crosslinking reaction process. More interestingly, TEM micrographs show that magnetic nanoparticles can be effectively adsorbed outside co-oligomeric particle cores in each nanocomposite (Runs 9–13), as shown in Figure 6.

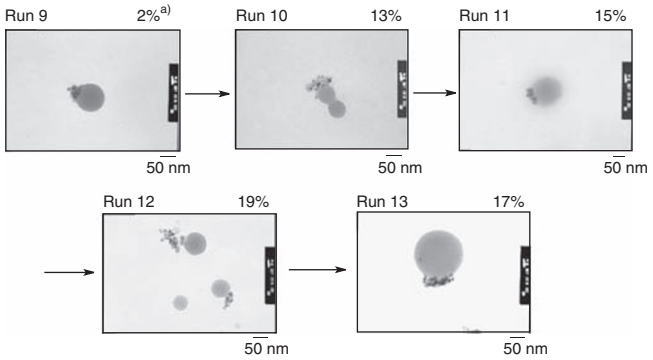

Figure 6 TEM photographs of **Magnt** adsorbed on fluorinated betaine-type co-oligomeric nanocomposites in methanol. *Each different from those of Table 3. **Content of **Magnt** in the composites determined by thermogravimetric analyses.

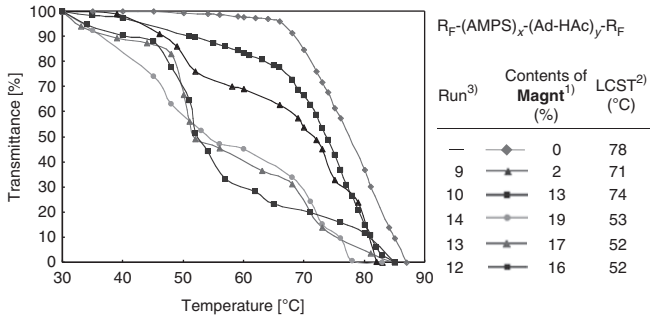

Figure 7 Temperature dependence of transmittance at 500 nm for *t*-butyl alcohol solutions of 4 g dm^{-3} R_F-(AMPS)$_x$-(Ad-HAc)$_y$-R_F co-oligomeric nanocomposite-encapsulated **Magnt**. (1) Contents of **Magnt** in nanocomoposites were determined by thermogravimetric analyses. (2) Defined by temperature when transmittance was 50%. (3) Each different from those in Table 3.

The LCST characteristic of novel crosslinked fluoroalkyl end-capped betaine-type co-oligomeric nanocomposite-encapsulated magnetic nanoparticles in organic media

It is well known that block copolymers such as poly(*N*-isopropylacrylamide)-*block*-poly(ethylene oxide) can exhibit thermosensitive micellization arising from a combination of the hydrophobic character of the poly(*N*-isopropylacrylamide) block above its LCST and the hydrophilic property of the poly(ethylene oxide) block in aqueous systems.[50,51] In contrast, fluoroalkyl end-capped betaine-type co-oligomeric nanoparticles containing adamantane segments can exhibit LCST behavior in organic media such as *t*-butyl alcohol because of the effective oleophilic–oleophobic balance between the oleophilic character from adamantyl segments and the oleophobic character from end-capped fluoroalkyl groups.[43,44] This is the first example of LCST behavior in organic media, although the LCST behavior of hydrocarbon polymers in ionic liquids has been previously reported by Watanabe *et al*.[52] Thus, it is of particular interest to study the LCST behavior of our present fluoroalkyl end-capped betaine-type co-oligomeric nanocomposite-encapsulated **Magnt** in organic media.

We measured the size of fluorinated betaine-type co-oligomeric nanocomposite-encapsulated **Magnt** by the use of DLS in *t*-butyl alcohol at temperatures ranging from 40 to 80 °C. The size of each fluorinated nanocomposite-encapsulated **Magnt** was found to increase from 17–18 nm to 26–33 nm when the temperature was increased from 40 to 80 °C, indicating that each nanocomposite-encapsulated **Magnt** causes thermally induced phase transition in *t*-butyl alcohol. In fact, *t*-butyl alcohol solutions of fluorinated betaine-type co-oligomeric nanocomposite-encapsulated **Magnt** exhibited a cloud point when heated from 30 to approximately 80 °C. The LCST values of *t*-butyl alcohol solutions with concentrations of 4 g dm^{-3} of the nanocomposites in Table 3 were measured, and results are shown in Figure 7.

A phase separation in each nanocomposite was found to occur between 52 and 74 °C, at which point the solubility of the nanocomposites altered sharply. The relationship between LCSTs and the **Magnt** content in the nanocomposites is shown in Figure 7.

The encapsulation of **Magnt** into fluorinated betaine-type co-oligomeric nanoparticles can effectively decrease the LCST from 78 to approximately 52 °C. The LCSTs were found to decrease with an increase in **Magnt** content in the nanocomposite particles. Above a content of 16%, the LCST remained nearly constant. Such an effective decrease in LCST by the encapsulation of **Magnt** is due to the magnetic interaction in each fluorinated nanocomposite particle. We believe that this is the first example of effective LCST control governed by the magnetic interaction derived from nanocomposite-encapsulated **Magnt**.

CONCLUSION

In summary, we succeeded in preparing novel crosslinked fluorinated co-oligomeric nanocomposite-encapsulated **Magnt**. The fluorinated nanocomposite-encapsulated **Magnt** particles were applied as a surface modification to PMMA and exhibited not only good oleophobicity imparted by the end-capped fluoroalkyl groups but also magnetic properties related to the **Magnt** in the composites. We also succeeded in preparing novel fluorinated betaine-type co-oligomeric nanocomposite-encapsulated **Magnt** under very mild conditions. These fluorinated nanocomposite-encapsulated **Magnt** particles were found to exhibit LCST behavior in *t*-butyl alcohol, and the magnetic interaction present effectively decreased LCST compared with parent fluorinated betain-type co-oligomeric nanoparticles without **Magnt**. Moreover, it was demonstrated that magnetic nanoparticles can be encapsulated inside the crosslinked fluorinated co-oligomeric nanoparticle cores. In contrast, magnetic nanoparticles were adsorbed outside the fluorinated betaine-type co-oligomeric nanoparticle cores. In this way, the fluorinated co-oligomers/**Magnt** nanocomposites that we present in this study have high potential for use in new fluorinated polymeric functional materials, serving as surface modifications of wallpaper and textiles, allowing for surface-active characteristics imparted by fluorine, as well as magnetic properties.

SUPPORTING INFORMATION

Thermogravimetric analyses of R_F-(IEM)$_x$-(Ad-HAc)$_y$-R_F co-oligomeric nanocomposite-encapsulated **Magnt**, X-ray diffraction patterns of R_F-(IEM)$_x$-(Ad-HAc)$_y$-R_F co-oligomeric nanocomposite-encapsulated **Magnt**, Fourier transform infrared spectra of R_F-(IEM)$_x$-(Ad-HAc)$_y$-R_F co-oligomeric nanocomposite-encapsulated **Magnt**, ultraviolet-visible spectral changes of the absorption at λ=500 nm of methanol solutions containing R_F-(IEM)$_x$-(Ad-HAc)$_y$-R_F co-oligomeric nanocomposite-encapsulated **Magnt** as a function of time, thermogravimetric analyses of R_F-(AMPS)$_x$-(Ad-HAc)$_y$-R_F nanocomposite-encapsulated **Magnt**, size of R_F-(AMPS)$_x$-(Ad-HAc)$_y$-R_F co-oligomeric nanocomposite-encapsulated **Magnt** in *t*-butyl alcohol solutions determined by dynamic light-scattering measurements and photographs of *t*-butyl alcohol solutions of R_F-(AMPS)$_x$-(Ad-HAc)$_y$-R_F co-oligomeric nanocomposite-encapsulated **Magnt** possessing the LCST characteristic are provided in the Supplementary Information.

ACKNOWLEDGEMENTS

We gratefully acknowledge the financial support from a grant-in-aid for Scientific Research from the Ministry of Education, Science, Sports and Culture, Japan. We also thank the Toda Kogyo Corporation (Hiroshima, Japan), Idemitsu Kosan, and Showa Denko for supplying magnetic nanoparticles, Ad-HAc and IEM-BO, respectively.

1 Huber, D. L. Synthesis, properties, & applications of iron nanoparticles. *Small* **1,** 482–501 (2005).
2 Roger, J., Pons, J. N., Massart, R., Halbreich, A. & Bacri, J. C. Some biomedical applications of ferrofluids. *Eur. Phys. J. Apply. Phys.* **5,** 321–325 (1999).
3 Speliotis, D. E. Magnetic recording beyond the first 100 years. *J. Magn. Magn. Mater.* **193,** 29–35 (1999).
4 Coey, J. M. D. Whither magnetic materials? *J. Magn. Magn. Mater.* **196–197,** 1–7 (1999).
5 O'Grady, K. & Laidler, H. The limits to magnetic recording—media considerations. *J. Magn. Magn. Mater.* **200,** 616–633 (1999).
6 Tofail, S. A. M., Rahman, I. Z. & Rahman, M. A. Patterned nanostructured arrays for high-density magnetic recording. *Appl. Organometal. Chem.* **15,** 373–382 (2001).
7 Perez, J. M., Simeone, F. J., Tsourkas, A., Josephson, L. & Weissleder, R. Peroxidase substrate nanosensors for MR imaging. *Nano Lett.* **4,** 119–122 (2004).
8 Hafeli, U. O. Magnetically modulated therapeutic systems. *Int. J. Pharma.* **277,** 19–24 (2004).
9 Bornscheuer, U. T. Immobilizing enzymes: how to create more suitable biocatalysts. *Angew. Chem. Int. Ed. Eng.* **42,** 3336–3337 (2003).
10 Kim, J., Lee, J. D., Na, H. B., Kim, B. C., Youn, J. K., Kwak, J. H., Moon, K., Lee, E., Kim, J., Park, J., Dohnalkova, A., Park, H. G., Gu, M. B., Chang, H. N., Grate, J. W. & Hyeon, T. A magnetically separable, highly stable enzyme system based on nanocomposites of enzymes and magnetic nanoparticles shipped in hierarchically ordered, mesocellular, mesoporous silica. *Small* **1,** 1203–1207 (2005).
11 Yoshino, T., Hirabe, H., Takahashi, M., Kuhara, M., Takeyama, H. & Matsunaga, T. Magnetic cell separation using nano-sized bacterial magnetic particles with reconstructed magnetosome membrane. *Biotech. Bioeng.* **101,** 470–477 (2008).
12 Dobson, J. Magnetic nanoparticles for drug delivery. *Drug Develop. Res.* **67,** 55–60 (2006).
13 Kim, J., Lee, J. E., Lee, S. H., Yu, J. H., Lee, J. H., Park, T. G. & Hyeon, T. Designed fabrication of a multifunctional polymer nanomedical platform for simultaneous cancer-targeted imaging and magnetically guided drug delivery. *Adv. Mater.* **20,** 478–483 (2008).
14 Hu, S.- H., Liu, D.- M., Tung, W.- L., Liao, C.- F. & Chen, S.- Y. Surfactant-free, self-assembled PVA-iron oxide/silica core-shell nanocarriers for highly sensitive, magnetically controlled drug release and ultrahigh cancer cell uptake efficiency. *Adv. Funct. Mater.* **18,** 2946–2955 (2008).
15 Wuang, S. C., Neoh, K. G., Kang, E.- T., Pack, D. W. & Leckband, D. E. Heparinized magnetic nanoparticles: *in-vitro* assessment for biomedical applications. *Adv. Funct. Mater.* **16,** 1723–1730 (2006).
16 Salgueirino-Maceira, V. & Correa-Duarte, M. A. Increasing the complexity of magnetic core/shell structured nanocomposites for biological applications. *Adv. Mater.* **19,** 4131–4144 (2007).
17 Shi, D., Cho, H. S., Chen, Y., Xu, H., Gu, H., Lian, J., Wang, W., Liu, G., Huth, C., Wang, L., Ewing, R. C., Budko, S., Pauletti, G. M. & Dong, Z. Fluorescent polystyrene-Fe_3O_4 composite nanospheres for *in vivo. Imaging and Hyperthermia.* **21,** 2170–2173 (2009).
18 Lin, P.- C., Chou, P.- H., Chen, S.- H., Liao, H.- K., Wang, K.- Y., Chen, Y.- J. & Lin, C.- C. Ethylene glycol-protected magnetic nanoparticles for a multiplexed immunoassay in human plasma. *Small* **2,** 485–489 (2006).
19 Srinivasan, B. & Huang, X. Functionalization of magnetic nanoparticles with organic molecules: loading level determination and evaluation of linker length effect on immobilization. *Chirality* **20,** 265–277 (2008).
20 Li, L., He, X., Chen, L. & Zhang, Y. Preparation of core-shell magnetic molecularly imprinted polymer nanoparticles for recognition of bovine hemoglobin. *Chem. Asian J.* **4,** 286–293 (2009).
21 Gao, J., Li, L., Ho, P.- L., Mak, G. C., Gu, H. & Xu, B. Combining fluorescent probes and biofunctional magnetic nanoparticles for rapid detection of bacteria in human blood. *Adv. Mater.* **18,** 3145–3148 (2006).
22 Sohn, B. H. & Cohen, R. E. Processible optically transparent block copolymer films containing superparamagnetic iron oxide nanoclusters. *Chem. Mater.* **9,** 264–269 (1997).
23 Lindlar, B., Boldt, M., Eiden-Assmann, S. & Maret, G. Synthesis of monodisperse magnetic methacrylate polymer particles. *Adv. Mater.* **14,** 1656–1658 (2002).
24 Flesch, C., Unterfinger, Y., Bourgeat-Lami, E., Duguet, E., Delaite, C. & Dumas, P. Poly(ethylene glycol) surface coated magnetic particles. *Macromol. Rapid Commun.* **26,** 1494–1498 (2005).
25 Wang, W.- C., Neoh, K.- G. & Kang, E.- T. Surface functionalization of Fe_3O_4 magnetic nanoparticles via RAFT-mediated graft polymerization. *Macromol. Rapid Commun.* **27,** 1665–1669 (2006).
26 Garcia, I., Zafeiropoulos, N. E., Janke, A., Tercjak, A., Eceiza, A., Stamm, M. & Mondragon, I. Functionalization of iron oxide magnetic nanoparticles with poly(methyl methacrylate) brushes via grafting-from atom transfer radical polymerization. *J. Polym. Sci. Part A: Polym. Chem.* **45,** 925–932 (2007).
27 Qiu, G., Wang, Q. & Nie, M. Polypyrrole-Fe_3O_4 magnetic nanocomposite prepared by ultrasonic irradiation. *Macromol. Mater. Eng.* **291,** 68–74 (2006).
28 Song, G., Bo, J. & Guo, R. The characterization and property of polystyrene compounding of α-Fe_2O_3 in the nano-scale. *Colloid Polym. Sci.* **282,** 656–660 (2004).
29 Dumazet-Bonnamour, I. & Perchec, P. L. Colloidal dispersion of magnetite nanoparticles via *in situ* preparation with sodium polyoxyalkylene di-phosphonates. *Colloid Surfaces A: Phys. Eng. Aspects* **173,** 61–71 (2000).
30 Kryszewskia, M. & Jeszkab, J. K. Nanostructured conducting polymer composites—superparamagnetic particles in conducting polymers. *Synthetic Metals* **94,** 99–104 (1998).
31 Nguyen, M. T. & Diaz, A. F. A novel method for the preparation of magnetic nanoparticles in a polypyrrole powder. *Adv. Mater.* **6,** 858–860 (1994).
32 Imae, T. Fluorinated polymers. *Curr. Opinion Colloid Interface Sci.* **8,** 307–314 (2003).
33 Yoshioka, H., Suzuki, M., Mugisawa, M., Naitoh, N. & Sawada, H. Synthesis and applications of novel fluorinated dendrimer-type copolymers by the use of fluoroalkanoyl peroxide as a key intermediate. *J. Colloid Interface Sci.* **308,** 4–10 (2007).
34 Yoshioka, H., Narumi, T. & Sawada, H. Synthesis of novel cross-linked fluorinated cooligomeric nanoparticles: synthetic approach to colloidal stable fluorinated magnetic nanocomposites. *J. Oleo Sci.* **56,** 377–383 (2007).
35 Yoshioka, H., Ohnishi, K. & Sawada, H. Preparation of fluoroalkyl end-capped oligomers/magnetite nanocomposites possessing a good dispersibility. *J. Fluorine Chem.* **128,** 1104–1111 (2007).
36 Sawada, H., Yoshioka, H., Kawase, T., Ueno, K. & Hamazaki, K. Preparation of magnetic nanoparticles by the use of self-assembled fluorinated oligomeric aggregates—a new approach to the dispersion of magnetic particles above poly(methyl methacrylate) film surface. *J. Fluorine Chem.* **126,** 914–917 (2005).
37 Sawada, H. Fluorinated peroxides. *Chem. Rev.* **96,** 1779–1808 (1996).
38 Sawada, H. Architechture and applications of novel self-assembled aggregates of fluoroalkyl-end-capped oligomers. *J. Fluorine Chem.* **101,** 315 (2000).
39 Sawada, H. Synthesis of self-assembled fluoroalkyl end-capped oligomeric aggregates—applications of these aggregates to fluorinated oligomeric nanocomposites. *Prog. Polym. Sci.* **32,** 509–533 (2007).
40 Sawada, H. Development of fluorinated polymeric functional materials using fluorinated organic peroxide as key material. *Polym. J.* **39,** 637–650 (2007).
41 Mugisawa, M., Ueno, K., Hamazaki, K. & Sawada, H. Synthesis and properties of novel cross-linked fluoroalkyl end-capped oligomeric nanoparticles containing adamantane units. *Macromol. Rapid Commun.* **28,** 733–739 (2007).
42 Mugisawa, M., Kasai, R. & Sawada, H. Cross-linked fluoroalkyl end-capped cooligomeric nanoparticle-encapsulated fullerene—a new approach to the surface modification of traditional organic polymers with fullerene-containing nanoparticles. *Langmuir* **25,** 415–421 (2009).
43 Mugisawa, M., Ohnishi, K. & Sawada, H. Preparation of novel fluoroalkyl end-capped 2-acrylamide-2-methylpropanesulfonic acid cooligomeric nanoparticles containing adamantane units possessing a lower critical solution temperature (LCST) characteristic in organic media. *Langmuir* **23,** 5848–5851 (2007).
44 Mugisawa, M. & Sawada, H. Architecture of linear arrays of fluorinated cooligomeric nanocomposites-encapsulated gold nanoparticles: a new approach to the development of gold nanoparticles possessing an extremely red-shifted absorption characteristic. *Langmuir* **24,** 9215–9218 (2008).
45 Liao, M.- H., Wu, K.- Y. & Chen, D.- H. Fast removal of basic dyes by a novel magnetic nano-adsorbent. *Chem. Lett.* **32,** 488–489 (2003).
46 Mak, S.- Y. & Chen, D.- H. Binding and sulfonation of poly(acrylic acid) on iron oxide nanoparticles: a novel, magnetic, strong acid cation nano-adsorbent. *Macromol. Rapid Commun.* **26,** 1567–1571 (2005).
47 Joumaa, N., Toussay, P., Lansalot, M. & Elaissari, A. Surface modification of iron oxide nanoparticles by a phosphate-based macromonomer and further encapsulation into submicrometer polystyrene particles by miniemulsion polymerization. *J. Polym. Sci. Part A: Polym. Chem.* **46,** 327–340 (2008).
48 Matsuno, R., Yamamoto, K., Otsuka, H. & Takahara, A. Polystyrene-grafted magnetite nanoparticles prepared through surface-initiated nitroxyl-mediated radical polymerization. *Chem. Mater.* **15,** 3–5 (2003).
49 Matsuno, R., Yamamoto, K., Otsuka, H. & Takahara, A. Polystyrene- and poly(3-vinylpyridine)-grafted magnetite nanoparticles prepared through surface-initiated nitroxide-mediated radical polymerization. *Macromolecules* **37,** 2203–2209 (2004).
50 Topp, M. D. C., Dijkstra, P. J., Talsma, H. & Feijen, J. Thermosensitive micelle-forming block copolymers of poly(ethylene glycol) and poly(N-isopropylacrylamide). *Macromolecules* **30,** 8518–8520 (1997).
51 Lin, H.- H. & Cheng, Y.- L. *In-situ* thermoreversible gelation of block and star copolymers of poly(ethylene glycol) and poly(N-isopropylacrylamide) of varying architectures. *Macromolecules* **34,** 3710–3715 (2001).
52 Ueki, T. & Watanabe, M. Lower critical solution temperature behavior of linear polymers in ionic liquids and the corresponding volume phase transition of polymer gels. *Langmuir* **23,** 988–990 (2007).

Supplementary Information accompanies the paper on Polymer Journal website (http://www.nature.com/pj)